Science of the Total Environment 891 (2023) 164385

Contents lists available at ScienceDirect

Science of the Total Environment

journal homepage: www.elsevier.com/locate/scitotenv

Comparative study on removal of platinum cytostatic drugs at trace level by cysteine, diethylenetriamino functionalized Si-gels and polyethyleneimine functionalized sponge: Adsorption performance and mechanisms

Dong Han [a], Montserrat López-Mesas [a,*], Markel Luaces [b], Yusleydi Enamorado [b], Martina Sanadar [c], Andrea Melchior [c], Manuel Valiente [a]

[a] GTS-UAB Research Group, Department of Chemistry, Faculty of Science, Universitat Autònoma de Barcelona, Bellaterra, (Cerdanyola del Vallès), 08193 Barcelona, Spain
[b] Faculty of Chemistry, University of Havana, 10400 Havana, Cuba
[c] Dipartimento Politecnico di Ingegneria e Architettura, Università di Udine, via del Cotonificio 108, 33100 Udine, Italy

HIGHLIGHTS

- Adsorption of emerging contaminants Pt-cytostatics using functionalized materials
- Effective elimination of trace concentrations of cisplatin and carboplatin
- Removal of Pt-cytostatics from hospital wastewater analogs
- Explanation of the adsorption mechanisms of different Pt compounds
- Enhanced adsorption *via* complexation between Pt-cytostatics and thiol groups

GRAPHICAL ABSTRACT

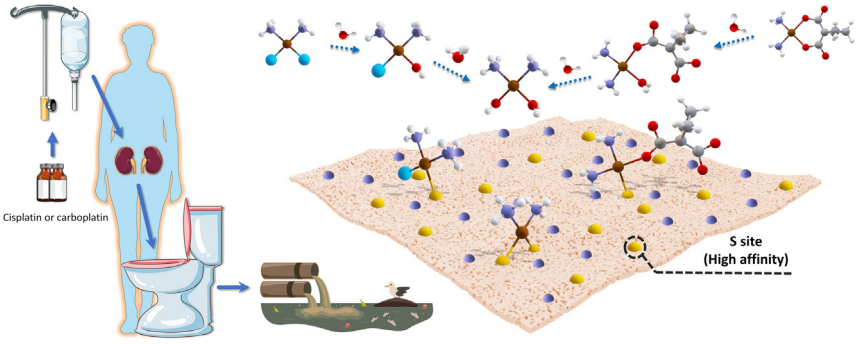

ARTICLE INFO

Editor: Damia Barcelo

Keywords:
Platinum cytostatics
Adsorption
Cisplatin
Carboplatin
Functionalized adsorbents

ABSTRACT

To efficiently remove trace Pt-based cytostatic drugs (Pt-CDs) from aqueous environments, a comparative investigation was conducted on the adsorption behavior of three commercial adsorbents including cysteine-functionalized silica gel (Si-Cys), 3-(diethylenetriamino) propyl-functionalized silica gel (Si-DETA) and open-celled cellulose MetalZorb® sponge (Sponge). The research on the adsorption of cisplatin and carboplatin encompasses investigations of pH dependence, adsorption kinetics, adsorption isotherms, and adsorption thermodynamics. The obtained results were compared with those of $PtCl_4^{2-}$ to better understand the adsorption mechanisms. The adsorption of cisplatin and carboplatin by Si-Cys was significantly better than Si-DETA and Sponge, which suggested that in chelation-dominated chemisorption, thiol groups provided high-affinity sites for Pt(II) complexation. Adsorption of the anion $PtCl_4^{2-}$ was more pH dependent and generally superior to that of cisplatin and carboplatin, benefiting from the contribution of ion association with protonated surfaces. The removal process of aqueous Pt(II) compounds occurred by the hydrolysis of complexes in solution and subsequent adsorption, and the specific adsorption process was explained by the synergistic action of ion association and chelation mechanisms. The rapid adsorption processes involving diffusion and chemisorption were well described by pseudo-second-order kinetic model. The isotherm studies suggested monolayer adsorption, consistent with the Langmuir model. Indicated from the adsorption enthalpy results, the chelation of cisplatin and carboplatin with thiol groups was an endothermic reaction, while the adsorption of $PtCl_4^{2-}$ was exothermic. At 343 K, Si-Cys achieved 98.5 ± 0.1 % (cisplatin) and 94.1 ± 0.1 % (carboplatin) removal. To validate the

* Corresponding author.
E-mail addresses: Dong.Han@uab.cat (D. Han), montserrat.lopez.mesas@uab.cat (M. López-Mesas).

http://dx.doi.org/10.1016/j.scitotenv.2023.164385
Received 21 March 2023; Received in revised form 16 May 2023; Accepted 20 May 2023
Available online 25 May 2023

obtained findings, the described process was applied to urine samples doped with Pt-CDs as analog of hospital wastewaters and the removal was very efficient, ranging from 72 ± 1 % to 95 ± 1 %, when using Si-Cys as adsorbent, although limited matrix effects were observed.

1. Introduction

Cisplatin (*cis*-diamminedichloroplatinum (II)) and carboplatin (1,1-cyclobutanedicarboxylatodiammineplatinum (II)), both well-known cytostatic agents, are administered intravenously to treat various types of cancers, including sarcomas, carcinomas, and germ cell tumors (Loehrer, 1984; Prestayko et al., 1979; Zamble and Lippard, 1995). Pharmacokinetic studies revealed that approximately 10–40 % of total Pt administered is excreted in the urine within 24 h, in the form of intact cisplatin which accounts for the majority of Pt excreted within 1 h of administration, or their metabolites and transformation products (Hann et al., 2003; Hoffmann-La Roche, 2020; Schmidt, 2019). These Pt compounds end up in hospital wastewater. Additionally, as a result of more frequent outpatient treatments, domestic discharge has become another considerable contribution of excreted Pt compounds, which is directly and inevitably discharged into municipal wastewater (Gouveia et al., 2023). Several studies, by means of advanced analytical methods, has shown the emergence of Pt-CDs in different water matrices (Ghafuri et al., 2018; Ghafuria et al., 2018; Isidori et al., 2016; Johnson et al., 2013; Kümmerer et al., 1999; Lenz et al., 2007a; Lenz et al., 2007b; Lenz et al., 2005; Roque-Diaz et al., 2021; Santana-Viera et al., 2020). European-wide investigations have found Pt compounds at concentrations ranging from tens of ng L^{-1} to a few hundred μg L^{-1} in hospital wastewaters (Ghafuria et al., 2018; Isidori et al., 2016; Kümmerer et al., 1999; Lenz et al., 2007a; Lenz et al., 2007b; Lenz et al., 2005; Santana-Viera et al., 2020; Vyas et al., 2014). Also, by analyzing samples from conventional wastewater treatment plants (WWTPs), it has been revealed that Pt concentration of municipal wastewater was one to three orders of magnitude lower than that of hospital wastewater (Ghafuri et al., 2018; Isidori et al., 2016; Santana-Viera et al., 2020). Through extensive dilution, it appears fortuitous that the concentration of Pt in surface waters remains consistently negligible and typically falls below the limit of detection (LODs), making its detection infrequent (Besse et al., 2012; Ghafuri et al., 2018; Isidori et al., 2016; Vyas et al., 2014). Regrettably, the hazardous Pt-CDs also have the potential to damage healthy cells within living organisms. The ecotoxicology and environmental risks of cisplatin or carboplatin have been assessed in recent years, and it can pose serious carcinogenic, teratogenic and mutagenic effects on exposed aquatic organisms (Araújo et al., 2019; Ghafuria et al., 2018; Heath and Isidori, 2020; Jureczko and Kalka, 2020; Li et al., 2021; Mišík et al., 2019; Queirós et al., 2021; Villarini et al., 2016; Yadav et al., 2021). In addition, the consequences of prolonged low-dose exposure might be underestimated and have not been fully characterized. Conventional WWTPs have been shown to be insufficient to effectively deal with this environmental threat due to the great challenges posed by the treatment of low-concentration Pt-CDs contaminated wastewater (Abdulbur-Alfakhoury et al., 2021; Heath and Isidori, 2020; Roque-Diaz et al., 2021).

This urgent environmental issue has raised concerns, and efforts have been made to explore potentially promising laboratory-scale treatments towards Pt-CDs contaminated wastewater (Roque-Diaz et al., 2021), including membrane bioreactor system (MBR) treatment (Lenz et al., 2007b), MBR coupled with adsorption and UV-treatment (Lenz et al., 2007a), and advanced oxidation process techniques (AOPs) (Hernández et al., 2008; Hirose et al., 2005; Kobayashi et al., 2008; Pieczyńska et al., 2017). Although these disposal methods have achieved certain effects, they are often accompanied by some shortcomings such as prolonged treatment time requirements, complicated installation and operation procedures, and high energy demands. Additionally, for example, after AOPs treatment, platinum by-products may still pose an environmental threat as heavy metal ions.

Compared with the aforementioned treatment methods, adsorption shows certain advantages over other technologies when considering the balance between economics, ease of operation and treatment efficiency. Moreover, adsorption demonstrates its applicability even at low concentrations of adsorbates, its capability in both batch and continuous processing modes, as well as the potential for recovery and regeneration of the adsorbent (Patel et al., 2019). Several adsorbent materials have been validated for their potential in the elimination of Pt-CDs (Dobrzynska et al., 2021; Farías et al., 2020; Folens et al., 2018; Fraguela et al., 2023; Lenz et al., 2005; Ogata et al., 2014). However, most of the previous adsorption experiments were carried out based on concentrations far higher than actual concentrations found in environments. For example, the newly reported low-cost adsorbent, Dithiocarbamate-Modified Silica (Fraguela et al., 2023), has achieved the effective removal of cisplatin in physiological conditions, but the study is based in concentration range > 5 mg L^{-1}. However, low Pt-CDs concentration will pose a challenge for efficient and fast adsorption, since small concentration gradients are insufficient to drive Pt compounds at the liquid-solid interface. Secondly, the reported adsorbents often require contact time of up to 24 h to reach equilibrium when adsorbing Pt compounds (Folens et al., 2018; Lenz et al., 2005; Ogata et al., 2014). The slow kinetic performance would not be conducive to scaling up the adsorption system to a column adsorption system and landing on a field application (Farías et al., 2020; Folens et al., 2018; Ogata et al., 2014). Some studies have initiated their adsorption investigations utilizing $PtCl_4^{2-}$ or $PtCl_6^{2-}$ as a preliminary model (Dobrzynska et al., 2021; Folens et al., 2018). However, it should be noted that the adsorption mechanism of these models may differ from that of the intended targets, and this aspect has been disregarded in said studies. For example, when adsorbents as biochar, chitosan, and granular activated carbon were used to adsorb cisplatin, carboplatin and oxaliplatin respectively, substantial differences from template $PtCl_6^{2-}$ in Pt recovery were already observed by authors (Folens et al., 2018). But these differences could not be well explained in detail. Interestingly, another material reported, Pt(II)-imprinted thiocyanato-functionalized SBA-15 (Dobrzynska et al., 2021) showed the similar removal effect as the template $PtCl_4^{2-}$ when adsorbing cisplatin, carboplatin and oxaliplatin but with achieving equilibrium in seven days. In conclusion, to address the above-mentioned issues, subsequent research needs to focus more on the adsorbents with strong affinity and high selectivity for Pt-CDs at trace concentrations in the environment. In turn, to achieve this goal, it is essential to explore and explain possible different adsorption mechanisms, especially in the face of diverse Pt-CDs.

This study first investigated the adsorption of cisplatin and carboplatin from aqueous solutions at trace concentrations typically present in real hospital wastewaters, using three commercially available adsorbents: cysteine-functionalized silica gel (Si-Cys), 3-(diethylenetriamino)propyl-functionalized silica gel (Si-DETA), and a derivatized open-celled MetalZorb® sponge (Sponge). Moreover, the adsorption of $PtCl_4^{2-}$, a compound with a structural similarity to cisplatin that has been widely utilized as a template in prior research, was also investigated for comparative purposes, with the differences in its intrinsic adsorption behavior being firstly elucidated. In detail, the influence of several parameters including pH, contact time, initial concentration, and temperature was studied.

2. Experimental methods

2.1. Materials

Potassium tetrachloroplatinate (II) (K_2PtCl_4, 99.9 %, CAS: 10025–99-7), diamminedichloroplatinum (II) (cisplatin, 99 %, CAS: 15663–27-1) and 1,1-cyclobutanedicarboxylatodiammineplatinum (II) (carboplatin,

99 %, CAS: 41575–94-4) were purchased from STREM Chemicals and were used without further purification. K_2PtCl_4, cisplatin and carboplatin stock solution (Pt concentration 100 mg L^{-1}) was initially prepared in 0.2 mol L^{-1} HCl respectively, and then diluted to the required concentration. Cysteine-functionalized silica gel (Si-Cys) and 3-(diethylenetriamino)propyl-functionalized silica gel (Si-DETA) were purchased from Sigma-Aldrich. MetalZorb® sponge (Sponge) was kindly supplied by CleanWay Environmental Partners, Inc. (Portland, USA). Details of the three commercial adsorbents are shown in Fig. S1(in Supplementary data). Milli-Q water (resistivity of 18.2 MΩ/m) was used throughout the entire experiment.

2.2. Preparation and characterization of adsorbents

Cube-shaped sponge (Fig. S1c, in Supplementary data) is an open-celled cellulose sponge that incorporates a water-insoluble polyamide chelating polymer formed by the reaction of polyethyleneimine and nitrilotriacetic acid. The sponge was claimed to contain free available ethyleneamine and iminodiacetate groups that could interact with heavy metals ions by ion exchange mechanism and chelation (Lou et al., 2022a; Lou et al., 2022b; Muñoz et al., 2002). These cubes were ground in a knife-milling commercial blender and sieved to a particle size of ≤0.5 mm. These fine sponge powders were washed with 1.0 mol L^{-1} HCl and Milli-Q water several times. Then the Sponge was dried at 80 °C for 24 h and stored for further studies.

To identify the functional groups of Si-Cys, Si-DETA, and Sponge, Fourier Transform Infrared Spectroscopy equipped with an Attenuated Total Reflectance module (ATR-FTIR, Tensor 27, Bruker, Germany) was used to record the FTIR spectra. The total content of C, H, N and S of three adsorbents was determined using element analyzer (Flash EA 2000 CHNS, Thermo Fisher, America). Brunauer-Emmett-Teller (BET) analysis results of Si-Cys and Si-DETA were provided by the manufacturer.

2.3. Batch adsorption

The adsorption of $PtCl_4^{2-}$, cisplatin and carboplatin was studied as a function of pH (pH 2–6, controlled by 0.1 mol L^{-1} HCl and/or 0.1 mol L^{-1} NaOH before, during, and after the adsorption, and monitored by pH meter, Crison, Spain), contact time (1–180 min), initial concentration (47 μg L^{-1} -1000 mg L^{-1}, all concentrations of Pt compounds are expressed as Pt), and solution temperature (293, 318 and 343 K). A series of batch adsorption experiments were performed in 10 mL plastic centrifuge tubes containing 10 mL of Pt solution (in form of $PtCl_4^{2-}$, cisplatin or carboplatin). After 50 mg of adsorbent was added, the tubes were agitated mechanically at 300 rpm at 293 K (except for thermodynamic studies). After 24 h (except for kinetic studies), the adsorbent in solution was filtrated using a 0.22 μm filter. The concentration of Pt in solutions was determined by Inductively Coupled Plasma Mass Spectrometry (ICP-MS, Thermo XSeries II, Thermo Scientific, USA).

The adsorption capacity q_e (μg g^{-1}) of Pt at equilibrium was calculated by the Eq. (1):

$$q_e = \frac{(c_0 - c_e)}{m} \times V \quad (1)$$

where c_0 and c_e (μg L^{-1}) are the initial and equilibrium concentrations of Pt solutions, respectively. V (mL) is the volume of solution and m (mg) is the adsorbent dosage. For kinetic studies, the concentration at equilibrium is replaced by the concentration at different contact time, c_t (μg L^{-1}), calculating the adsorption capacity q_t (μg g^{-1}).

Then the removal ratios were calculated according to Eq. (2):

$$\text{Removal ratio} = \frac{(c_0 - c_e)}{c_0} \times 100\% \quad (2)$$

All the experiments were conducted in triplicated, and the average values and the relative standard deviation were calculated.

2.4. Adsorption kinetic and isotherm modeling

To further understand the Pt adsorption behavior, kinetic models including pseudo-first-order model (PFOM) and pseudo-second-order model (PSOM) were used to fit the adsorption data collected at different contact time, while data obtained from different initial concentration were fitted with Langmuir and Freundlich isotherm models. The adsorption kinetic and isotherm equations are described in Supplementary data.

2.5. Experimental validation of the removal of Pt-CDs in wastewater analog samples

To validate the feasibility and efficiency of the Pt-CDs removal, experiments were carried out by using urine samples doped with Pt-CDs as hospital wastewater analogs. To this purpose, and due to the difficulty of obtaining hospital samples, hospital wastewater analogs were prepared from anonymous urine samples obtained from a healthy male spiked with cisplatin and carboplatin at the level of reported excreted in urine of patients undergoing chemotherapy (cisplatin concentration from 312.39 μg L^{-1} to 114.81 mg L^{-1}) (Jantarat et al., 2021). Then, these samples were diluted ten and 100-fold to account for typical conditions in hospital wastewaters. Ion chromatography (Dionex Aquion, Thermo Scientific, America) was employed to determine the concentration of typical anions and cations in urine and two wastewater analogs, and details are described in Supplementary data. Experiments were carried out by contacting the prepared analog samples with the adsorbent Si-Cys in the same conditions as explained when using the synthetic Pt-CDs solutions. Thus, 10 mL of the resulting Pt-spiked urine samples were then respectively mixed with 50 mg of the selected adsorbent (stirred for 24 h, T = 343 K, pH 2) and were collected using sterile plastic bottles after filtration using 0.22 μm filters. The samples were immediately quantified using a standard analytical method described elsewhere (Flores et al., 2011; Gao et al., 2012). In our case, analog samples aliquots (100 μL) were equilibrated to room temperature and digested using 200 μL of nitric acid (69.0–70.0 %, for trace metal analysis) at 363 K for 1 h. The digested samples were then diluted to 10 mL with Milli-Q water to a final concentration of 2 % v/v HNO_3. These solutions were instantly subjected to ICP-MS analysis with external calibration ranging from 1 to 150 μg L^{-1} (Rh and Y as internal standard elements). The calculation of removal ratio was according to Eq. (2).

3. Results and discussion

3.1. Characterization of adsorbents

The FTIR test was performed on Si-Cys, Si-DETA, and Sponge, showing the spectra observed in Fig. 1. The spectra of Si-Cys and Si-DETA are very similar, and the characteristic peaks mainly correspond to the properties of silica. Absorption bands at 1051 cm^{-1} and 795 cm^{-1} arise from asymmetric vibration of Si-O-Si and symmetric vibration of Si-O-Si, respectively (Grumezescu et al., 2014). The peaks at 2973 cm^{-1} and 2900 cm^{-1} represent the C—H stretching vibration of the alkyl groups. The broad band at around 3273 cm^{-1} was assigned to N—H stretching of amine, which was relatively weak due to low load rate of cysteine and 3-(diethylenetriamino) propyl groups. Then, the band appears at 1615 cm^{-1} for Si-Cys representing C═O stretching vibration. For Sponge, the absorbances at 3435, 2891, 1365, 1157, and 1024 cm^{-1} are associated with cellulose substrate (Li et al., 2009). A strong band 3435 cm^{-1} originates from the O—H stretching. The peak at 2891 cm^{-1} is attributed to the stretching vibration of alkane C—H. The absorption at 1365 cm^{-1} is due to O—H bending and that at 1157 cm^{-1} corresponds to C-O-C antisymmetric bridge stretching. The strong peak at 1024 cm^{-1} can be assigned to C-O-C pyranose ring skeletal vibration. Besides, the surface polyamide chelating polymer contributes to the strong band at around 3317 cm^{-1} due to the N—H stretching. The peak at 1637 cm^{-1} is related to the C═O stretching vibration and the rightward shift of the peak coincides with the amide structure (electron-donating property of nitrogen). These findings are consistent with

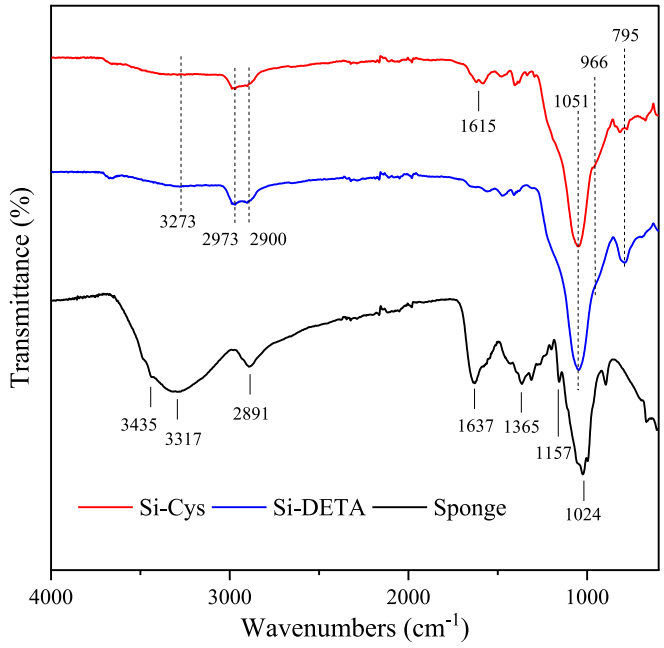

Fig. 1. FTIR spectra of Si-Cys, Si-DETA, and Sponge.

the interpretation of the chemical structure of the different adsorbents, shown in Fig. S1(in Supplementary data).

BET analysis and elemental analysis (EA) results are summarized in Table S1 and Table S2 (in Supplementary data), respectively. The EA analysis conducted confirmed the existence of the respective functional groups in the three adsorbents, which aligns with the FTIR findings and uphold the claims made by the manufacturers.

3.2. Adsorption experiments

3.2.1. Effect of solution pH on adsorption

The pH is one of the key factors that determine the interaction between adsorbate and adsorbent as it can change the protonation state of surface functional groups, thereby changing the surface charge, which in turn affects the adsorption performance. For adsorption of $PtCl_4^{2-}$ (Fig. 2a), the pH dependences of the three materials are very different. The adsorption capacity of Si-Cys decreased considerably from 45 ± 1 to 19 ± 4 μg g^{-1} as pH increased from 2 to 6. As implied in Fig. 3a, after dilution from Pt stock (in 0.2 mol L^{-1} HCl), the Cl ligands are gradually displaced by H_2O to give the aqua complexes (like $PtCl_3(H_2O)^-$). And at low pH values, the amino groups were protonated, which made the adsorbent to be positively charged. The protonation facilitated Si-Cys to attract anionic $PtCl_4^{2-}$ and/or $PtCl_3(H_2O)^-$ through ion association, concomitantly, Pt gradually chelated with the S sites and the N sites (even with low affinity). However, when the pH kept increasing, the carboxyl group, thiol group and protonated amine group sequentially deprotonated, which eventually caused Si-Cys to be negatively charged. Due to electrostatic repulsion, parts of $PtCl_4^{2-}$ and/or $PtCl_3(H_2O)^-$ molecules were repelled, as a result, there was a significant decrease in the adsorption capacity. Meanwhile, however, the changing of adsorption capacity with increasing pH was moderated when Si-DETA was studied, adsorption capacity of Si-DETA dropped slightly from 48 ± 1 to 42 ± 1 μg g^{-1} in the same range of pH. The elevation of pH levels induced deprotonation of amine groups in Si-DETA, resulting in a reduction of its positive charge density. As a consequence, the effectiveness of electrostatic attraction-assisted adsorption was moderately diminished. The effect of pH on the adsorption of $PtCl_4^{2-}$ to Sponge is almost negligible.

For cisplatin (Fig. 2b) and carboplatin (Fig. 2c), the adsorption capacities were overall lower than that of $PtCl_4^{2-}$ and slightly affected by pH changes, since facing cisplatin and carboplatin (neutral molecules) as well as their hydrated complexes (non-anionic molecules) electrostatic attraction did not contribute to the adsorption. Regarding the adsorbents, Si-Cys has higher adsorption capacities of cisplatin and carboplatin than Si-DETA and Sponge due to the presence of thiol groups in Si-Cys. According to HSAB theory (Bugarčić et al., 2012), Pt(II) as a "soft" acid has a high affinity for sulfur donors ("soft" bases) *e.g.* thiols and thioethers. For example, it is assumed that most of Pt-CDs bind to glutathione and L-cysteine in intracellular liquid forming stable compounds before it reaches DNA (Bugarčić et al., 2012; Reedijk, 2009; Reedijk, 1999). This suggests that in chelation-dominated chemisorption (Fig. 3b and c), thiol groups provide more chelation sites for the complexation of cisplatin and carboplatin.

In addition, it is worth mentioning here that the influence of the alkaline environment is not considered, because the chemical structures of $PtCl_4^{2-}$, cisplatin and carboplatin are not stable when the pH exceeds 6. Black precipitation appeared in both stocks prepared by directly dissolving compounds in water at pH > 6, due to the oxidation of Pt.

3.2.2. Adsorption kinetics analysis

Kinetic is an important index to evaluate the removal efficiency and mechanism of the adsorption process, that is a key knowledge to scale up the Pt-CDs removal to industrial application. Fig. 4A and a give the adsorption kinetic curves of $PtCl_4^{2-}$ onto Si-Cys, Si-DETA, and Sponge. It is shown a fast adsorption kinetics for all the three materials. The adsorption capacities rose sharply within the first few minutes, because there are rich effective adsorption sites on the surface of Si-Cys, Si-DETA, and Sponge at the beginning of the adsorption process. Then the growth gradually slowed down until reaching the adsorption equilibrium after approximately 40 min, as the amounts of available active sites gradually decreased, leading to a decrease in the adsorption rate. However, despite of the fast kinetics, the adsorption of cisplatin and carboplatin still exhibited disadvantages if compared to that of $PtCl_4^{2-}$(see in Fig. 4). The removal rate of Si-DETA and Sponge for cisplatin was only 32 ± 2 % and 38 ± 3 % (while 9 ± 1 % and 10 ± 2 % for carboplatin), compared to 90 ± 1 % and 83 ± 3 % for $PtCl_4^{2-}$. This confirmed the inference in the previous section that the adsorption was frustrated due to the lack of thiol groups to provide complexation sites. In addition, carboplatin showed worse adsorption performance, which was caused by its low hydrolysis rate. Meanwhile, the removal rate of Si-Cys also slightly decreased from 92 ± 1 % for $PtCl_4^{2-}$ to 74 ± 1 % for cisplatin and 73 ± 1 % for carboplatin, indicating that electrostatic adsorption probably did not play a role in adsorbing cisplatin and carboplatin molecules.

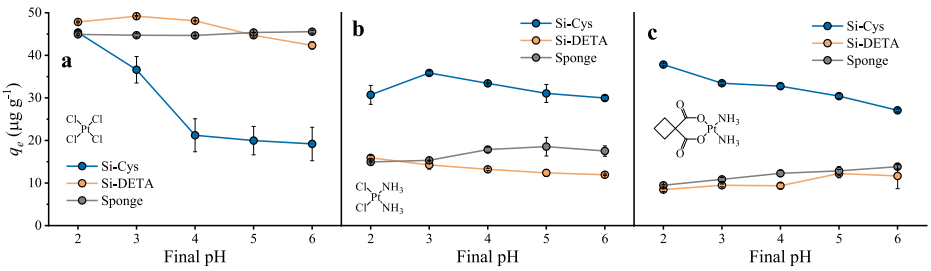

Fig. 2. The effect of solution pH on the adsorption capacity of (a) $PtCl_4^{2-}$, (b) cisplatin and (c) carboplatin [adsorbent dosage: 50 mg, solution volume: 10 mL, Pt concentration: 235 μg L^{-1}, T: 293 K].

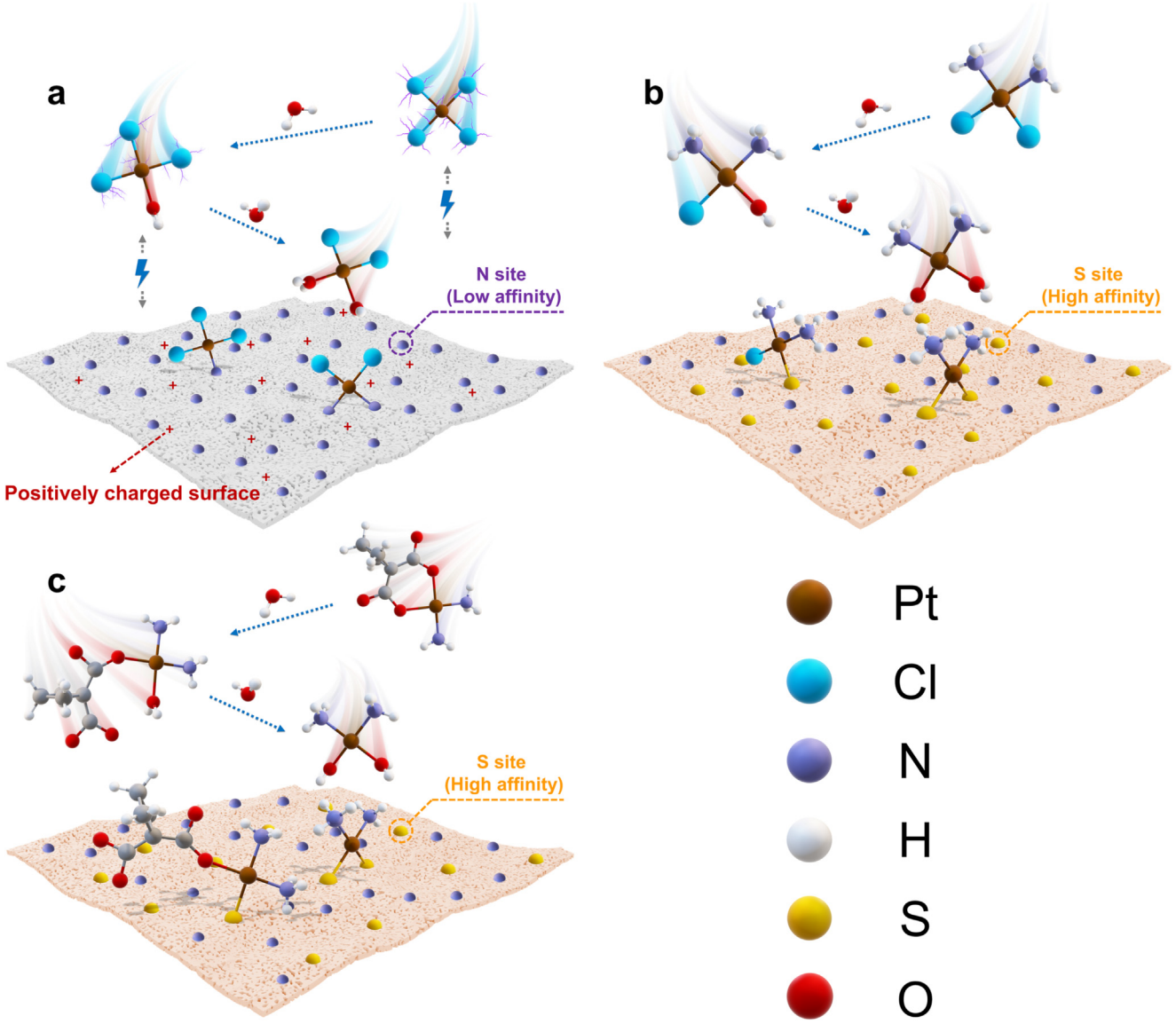

Fig. 3. The difference in adsorption mechanism between (a) $PtCl_4^{2-}$, ion association enhanced adsorption to amino-rich adsorbent surface (adsorption to Si-Cys containing thiol group is omitted here); (b) cisplatin and (c) carboplatin chelation dominant adsorption to thiol-containing Si-Cys surface.

The kinetics fitting curves are also plotted in Fig. 4. As indicated by the correlation coefficients R^2 summarized in Table S3 (in Supplementary data), PSOM fitted better than PFOM. As is known PSOM assumes that the rate-limiting step may be chemisorption involving valance forces through sharing or exchanging electrons between adsorbate and adsorbent (Feiqiang et al., 2018; Mohan et al., 2011; Sen Gupta and Bhattacharyya, 2011). Specifically, this is consistent with the ion-association between the $PtCl_4^{2-}$ anion and the protonated amine group, and the complexation between Pt and surface functional groups such as thiol, amino and carboxyl groups. Furthermore, it has been reported that the PFOM is more suitable for the description of the initial stage in which the external/internal diffusion is the rate controlling step, and the initial concentration of adsorbate is usually high (Feiqiang et al., 2018; Wang and Guo, 2020a). However, the initial concentration of the target Pt compounds here was as low as 235 μg L^{-1}, and the adsorbents are abundant with active sites, therefore, the adsorption kinetics are dominated by the adsorption onto active site as PSOM expected.

3.2.3. Adsorption isotherms analysis

Adsorption isotherm reveals the relationship between the adsorbate concentration in the liquid and solid phases when the adsorption process reaches equilibrium. Adsorption capacities mounted with the increase of the initial concentration of $PtCl_4^{2-}$, cisplatin and carboplatin solution (see in Fig. 5), which may be due to the higher concentration gradient at the solid-liquid interface. The mass transfer of $PtCl_4^{2-}$, cisplatin and carboplatin towards the surface of adsorbents could be driven by the concentration gradient, which satisfied the generalized Fick Law (Chinh et al., 2019; Han et al., 2021). It can be seen from Fig. 5A that the maximum adsorption capacity of Si-DETA (169 ± 6 mg g^{-1}) to $PtCl_4^{2-}$ is greater than that of Si-Cys (131 ± 1 mg g^{-1}), due to the different loading rates of their respective functional groups, -Cys (0.3 mmol g^{-1}) and -DETA (1.3 mmol g^{-1}) (provided by the manufacturer, see Fig. S1a and S1b, in Supplementary data). Moreover, the adsorption of $PtCl_4^{2-}$ surpasses that of the other two Pt compounds, ascribed to the complementary effect of electrostatic adsorption and Van der Waals force, alongside the presence of ligands (Cl) that readily detach from the molecule. Cisplatin and carboplatin contain two inert NH_3 ligands which makes complexation to the adsorbent surface more difficult. This predicament is slightly alleviated when Si-Cys containing thiol functional groups were used to adsorb cisplatin and carboplatin.

The isotherm fitting curves are also plotted in Fig. 5, and parameters derived from models are summarized in Table S4 (in Supplementary data). Langmuir model represents satisfactorily the adsorption process with high

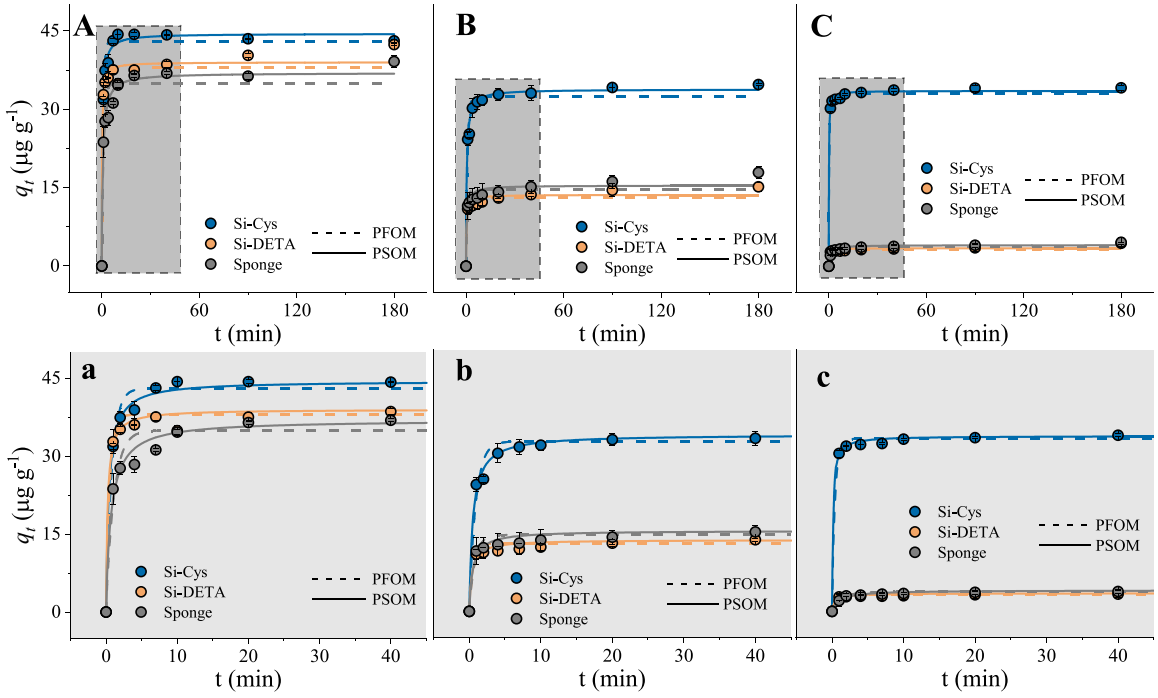

Fig. 4. The effect of contact time on the adsorption capacity of (A) $PtCl_4^{2-}$, (B) cisplatin and (C) carboplatin [adsorbent dosage: 50 mg, solution volume: 10 mL, Solution pH = 2 for Si-Cys and Si-DETA, solution pH = 3 for Sponge, Pt concentration: 235 μg L^{-1}, T: 293 K] and kinetic models fitting. The lowercase figures (gray background) are the enlarged interval (0–40 min).

coefficients of determination ($R^2 > 0.92$) and gives a better fit than Freundlich model only except for Si-Cys adsorption of cisplatin and Si-DETA adsorption of carboplatin (while Freundlich model fit is slightly better). The results indicate that the adsorption of three Pt compounds by all adsorbents takes place in a monolayer adsorption manner. In addition, the adsorption (Fig. 5a-c) in the low concentration range obeys the linear

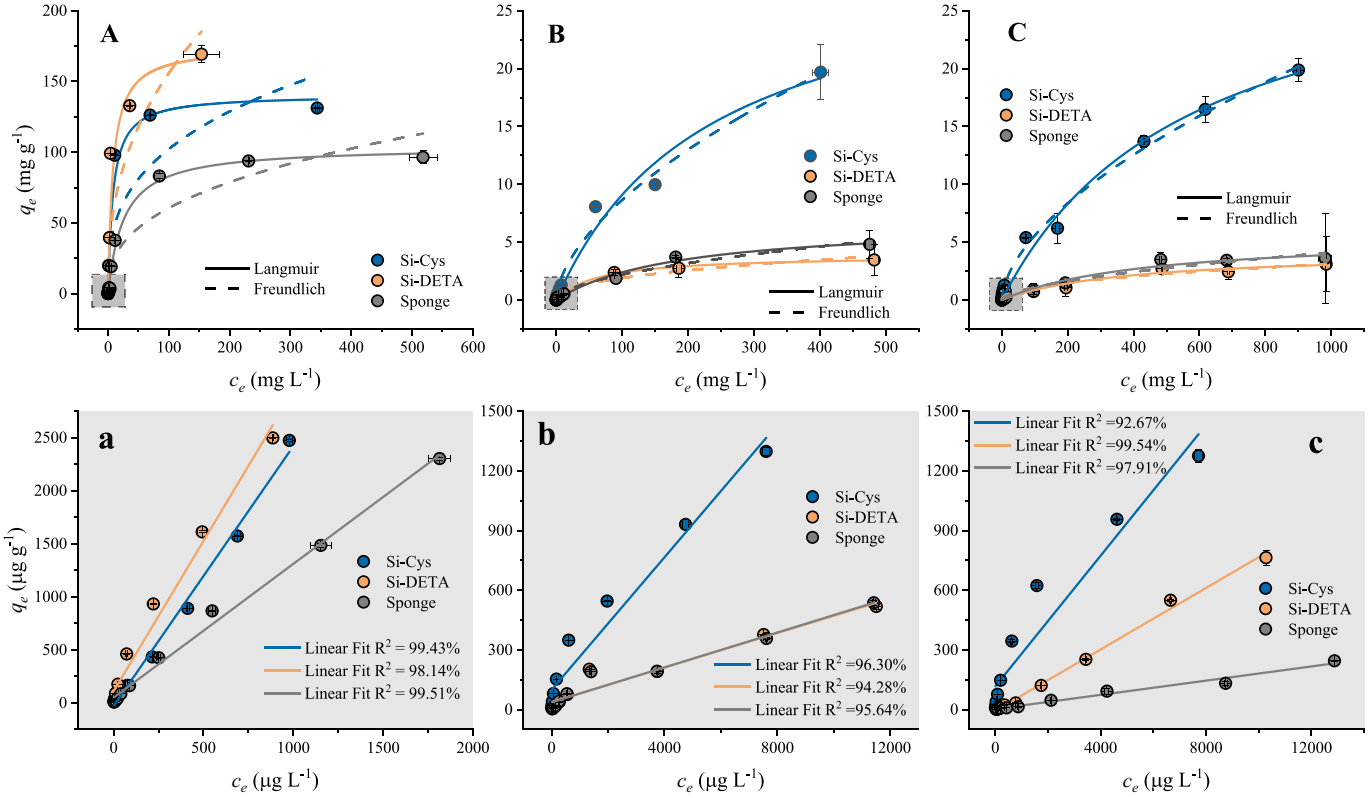

Fig. 5. Adsorption equilibriums of (A) $PtCl_4^{2-}$, (B) cisplatin and (C) carboplatin [adsorbent dosage: 50 mg; solution volume: 10 mL; initial concentration: maximum 1000 mg L^{-1} of $PtCl_4^{2-}$ and carboplatin, 500 mg L^{-1} of cisplatin because of low solubility; solution pH = 2 for Si-Cys and Si-DETA, solution pH = 3 for Sponge; contact time 24 h; T: 293 K] and isotherm models fitting. The lowercase figures (gray background) are the enlarged interval (initial concentration 47–14,100 μg L^{-1}).

model (Henry's law), which also illustrates the monolayer adsorption behavior with low coverage (Wang and Guo, 2020b). From the data listed in Table S4 (in Supplementary data), all the Langmuir separation factor R_L fell into 0 to 1 within the concentration range investigated. It proves that all Pt adsorptions towards three materials are favorable. The theoretical maximum adsorption q_m predicted by the Langmuir model is close to but slightly higher than the actual maximum adsorption capacity obtained in the experiment. Regarding the Freundlich constant, all adsorption processes are favorable as the value of $1/n < 1$.

3.2.4. Thermodynamics of adsorption processes

Experimental thermodynamic analysis was performed under different temperatures to further understand the adsorption behavior. For $PtCl_4^{2-}$ (see in Fig. 6A), with the increase of adsorption temperature (from 293 to 343 K), the adsorption capacities of Si-Cys, Si-DETA, and Sponge all decreased slightly. Then when initial concentrations doubled to 470 μg L^{-1}, the decline was more obvious (see in Fig. 6a). As illustrated in Fig. 3a, the adsorption of anionic $PtCl_4^{2-}$ was dominated by physical adsorption such as electrostatic attraction and Van der Waals forces. Specifically, the weak binding between $PtCl_4^{2-}$ and adsorbents surface caused by Van der Waals interactions, which are always present in adsorption processes (Veclani et al., 2020), were easily undermined as the solutions were heated up to 343 K. In comparison, the adsorption of cisplatin is much more complicated. As shown in Fig. 6B and b, the adsorption capacities of Si-Cys to cisplatin were greatly promoted when temperature was increased, and the removal rates almost reached the theoretical maximum at 343 K (98.5 ± 0.1 % and 97.5 ± 0.5 % for initial concentration of 235 and 470 μg L^{-1}, respectively). The adsorption process of carboplatin also showed a similar pattern. This implied that the chemisorption dominated by chelation was a thermophilic process, and the complexation between Pt and S from the thiol group was facilitated at higher temperatures during the process. However, for the other two adsorbents, Si-DETA and Sponge, the adsorption capacities of them for cisplatin and carboplatin were not only much lower than that of Si-Cys (electrostatic adsorption was ineffective for neutral cisplatin or carboplatin, and the complexation of Pt—N was weaker), they also showed a trend of increasing and then decreasing during the warming process (see in Fig. 6B,C and 6b,c). For instance, when the temperature increased from 293 K to 318 K, adsorption capacities of cisplatin on Si-DETA and Sponge generally increased (except for the adsorption of Si-DETA in Fig. 6b, which adsorption decreased by a very small amount of 1.66 μg L^{-1}), which was due to the high temperature promoting to some extent the complexation of Pt with the amine functional groups on the surface of Si-DETA and Sponge. However, as explained before, this complexation was very limited because of the fact that N is a "hard" base and its bonding with the "soft" acid Pt is not favored. Therefore, when the temperature continued to increase up to 343 K, the decline brought by the frustrated Van der Waals adsorption came to the fore.

Furthermore, three thermodynamic parameters including Gibbs free energy (ΔG°), enthalpy change (ΔH°), and entropy change (ΔS°) were calculated by equations described in Supplementary data. Results are listed in Table S5 (also in Supplementary data).

As seen in Table S5, $PtCl_4^{2-}$ adsorption is a spontaneous process with negative ΔG°. It can be seen from the comparison of ΔH° that the adsorption of $PtCl_4^{2-}$ by Si-Cys was very different from that of cisplatin or carboplatin. First, as can be determined from the positive value of ΔH°, the adsorption of cisplatin or carboplatin is endothermic reaction (while that of $PtCl_4^{2-}$ is exothermic). Additionally, cisplatin has an enthalpy value (ΔH° = 44 ± 7 kJ mol^{-1}) approximately twice as high as the ΔH° of $PtCl_4^{2-}$ (ΔH° = −23 ± 6 kJ mol^{-1}), which corroborates the dominance of chemisorption in the adsorption of cisplatin by Si-Cys. It can be recognized that temperature promoted bonding of Pt—S, and enthalpy change of this process was incontrovertibly higher than that involved in physisorption. In addition, the entropy changes of Si-Cys in the process of adsorbing $PtCl_4^{2-}$ and other two Pt-CDs are also diametrically opposite. Negative values of ΔS° indicated an increase in the order of the system during the adsorption process of $PtCl_4^{2-}$ at solid-liquid interface, while positive ΔS° suggested an increase of the degrees of freedom when cisplatin and carboplatin was adsorbed on Si-Cys.

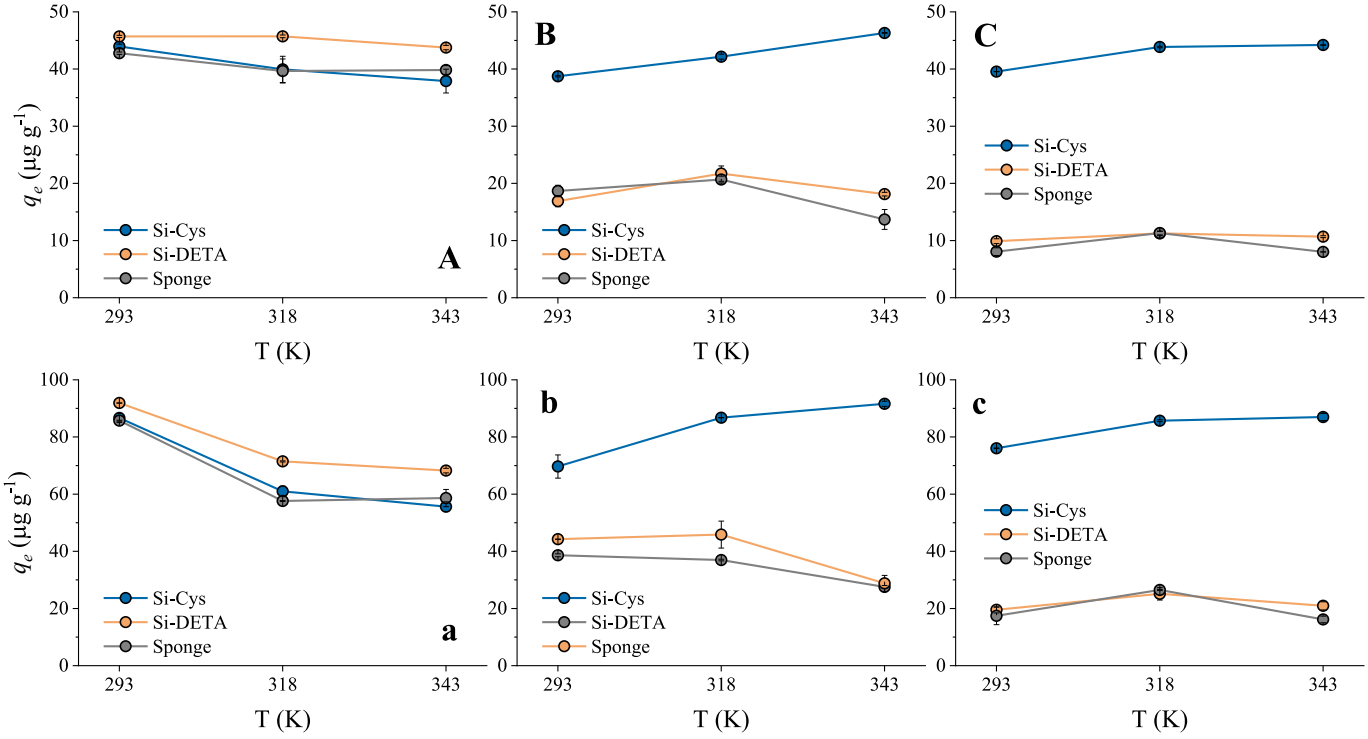

Fig. 6. The effect of temperature on the adsorption capacity of $PtCl_4^{2-}$, Pt concentration: (A) 235 μg L^{-1} and (a) 470 μg L^{-1}; cisplatin, Pt concentration: (B) 235 μg L^{-1} and (b) 470 μg L^{-1}; carboplatin, Pt concentration: (C) 235 μg L^{-1} and (c) 470 μg L^{-1}. [adsorbent dosage: 50 mg, solution volume: 10 mL, contact time: 24 h, Solution pH = 2 for Si-Cys and Si-DETA, solution pH = 3 for Sponge].

3.3. Experimental validation of the removal of Pt-CDs in wastewater analog samples

The results of the removal of Pt-CDs in wastewater analog samples are depicted in Fig. 7, and the characteristics of urine and wastewater analogs are summarized in Table S6 (in Supplementary data). It can be observed by comparing Fig. 7a and b, the Si-Cys adsorption towards the two targets generally achieved similar removal rates, which are from 72 ± 1 % to 95 ± 1 % for cisplatin and from 75 ± 1 % to 95 ± 1 % for carboplatin. The removal was found to be less efficient for low concentrations of cisplatin and carboplatin in undiluted urine samples, likely due to the complexity of the urine matrix (as Table S6 shows). Furthermore, the observed removal of Pt-CDs in simulated wastewaters was consistently lower than that in Milli-Q water. This disparity may be attributed to the matrix effect that arises from the presence of urine and tap water. One of its interferences may be derived from the trace protein contained in urine such as Tamm-Horsfall protein (Aitekenov et al., 2021; Micanovic et al., 2020), which contains cystines sites that pre-chelated part of cisplatin and carboplatin. Secondly, the ligands replacement of cisplatin and carboplatin could be disturbed due to the presence of components such as Cl^- and NH_4^+ in urine matrix, which were significantly more abundant than Pt-CDs as indicated in the Table S6, thus the complexation of Pt to the Si-Cys surface was also affected (Guo et al., 2020). In addition, co-existing ions such as Na^+, K^+, Ca^{2+} and so on (several to thousands of mg L^{-1}) present in urine posed additional competition for active binding therefore slightly inhibited the capture of cisplatin and carboplatin (Curtis et al., 2010). For the undiluted samples, the Pt species had more competitive advantages when the initial concentration was increased to 57 or 115 mg L^{-1}, hence the removal rates increased significantly driven by the high concentration gradients. The interference from matrix effects diminished gradually with more dilution of urine, almost all removals reached the maximum (92 ± 1 % - 95 ± 1 %) when adsorptions were carried out in 100-fold diluted urine samples. The only exception occurred in the adsorption of spiked low-concentration Pt from urine. When the urine samples were further diluted from ten times to 100 times, the removal rate decreased unexpectedly. However, the initial Pt concentration was as low as only 3.12 μg L^{-1}, which may predict the ineffective capture of Pt molecules at such a low concentration. Perhaps longer time or higher temperature can guarantee more Pt—S complexation formed for ideal adsorption.

Then when the mixture of cisplatin and carboplatin was adsorbed from 100-fold diluted urine, as shown in Fig. 7c, around 95 % of Pt was effectively removed. The removal of Pt-CDs from 100-fold diluted urine is comparable to that from Milli-Q water, albeit slightly lower.

3.4. Comparison of the adsorption performance with current knowledge

The adsorption efficiency of Si-Cys for cisplatin and carboplatin was compared with other published adsorbents and listed in Table 1. It is

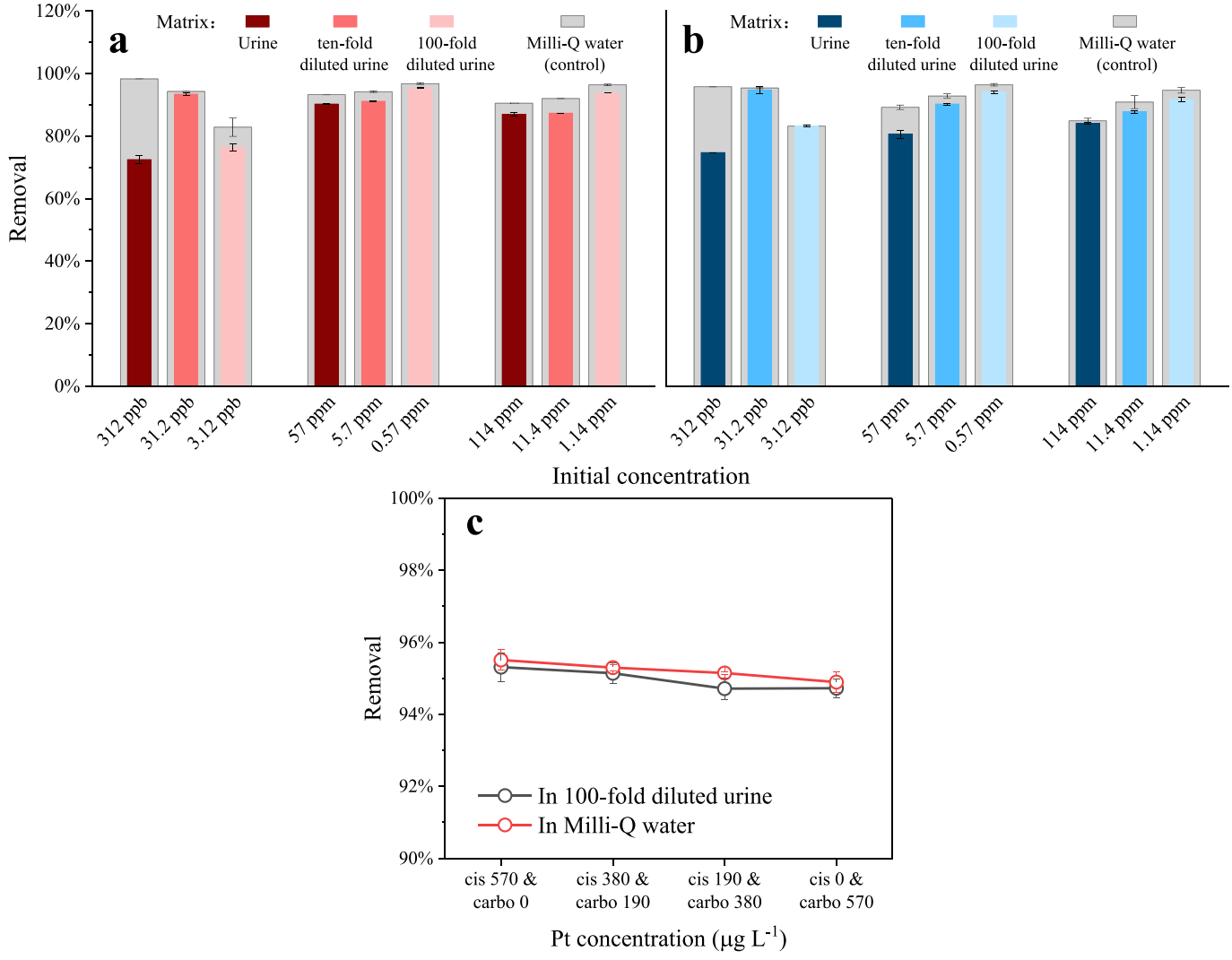

Fig. 7. Removal of (a) cisplatin and (b) carboplatin from spiked urine samples, its ten-fold diluted and 100-fold diluted matrices; (c) mixture of cisplatin and carboplatin from 100-fold diluted urine.

Table 1
Comparison of Pt-CDs removal by Si-Cys to adsorbents previously reported.

Adsorbent	Target Pt compound	Contact time (h)	Dosage (g L^{-1})	Treatment effect	Ref.
Si-Cys	Cisplatin (235 μg L^{-1} Pt) Carboplatin (235 μg L^{-1} Pt)	40 min	5.0	98.5 ± 0.1 % removal 94.1 ± 0.1 % removal	This study
Activated sludge	Cisplatin (6.5 μg L^{-1} Pt) Carboplatin (5.3 μg L^{-1} Pt) Oxaliplatin (4.9 μg L^{-1} Pt)	24	4.2	96 % removal 70 % removal 74 % removal	(Lenz et al., 2005)
Biomass-derived adsorbents (chitosan, biochar, wood ash, activated carbon)	$PtCl_6^{2-}$ as model (1–10 mg L^{-1} Pt)	24	10.0	Adsorption capacity 0.23–0.97 mg g^{-1}	(Folens et al., 2018)
Calcination of gibbsite	Cisplatin (10 mg L^{-1} Pt)	24	6.0	Adsorption capacity 1.5 mg g^{-1}	(Ogata et al., 2014)
Macroporous cryogels (by polymerization of methacrylic acid and 2-hydroxyethyl methacrylate)	Cisplatin (250–2000 mg L^{-1})	1–48	0.5 & 2.0	Adsorption capacity up to 150 mg g^{-1}	(Farías et al., 2020)
Pt (II)-imprinted thiocyanato-functionalized SBA-15 materials	$PtCl_4^{2-}$ as model (100 mg L^{-1} Pt)	5	5.0	Adsorption capacity 76.4 mg g^{-1}	(Dobrzynska et al., 2021)
Dithiocarbamate-Modified Silica	Cisplatin (10 mg L^{-1})	0.25–2	1–10	Adsorption capacity 15.6 mg g^{-1} with 1 mg mL^{-1}. Removal up to 85 % with 10 mg L^{-1}. 1 h contact time	(Fraguela et al., 2023)

evident that Si-Cys achieved maximum removal of 98.5 ± 0.1 % and 94.1 ± 0.1 % for cisplatin and carboplatin, respectively. Moreover, it was achieved at a low concentration of 235 μg L^{-1}, which is close to the environmental concentrations. Although activated sludge (Lenz et al., 2005) also exhibited good removal efficiency at low concentrations, the disadvantage of slow kinetics required a long processing time of up to 24 h. While it is acknowledged that novel adsorbents like macroporous cryogels (Farías et al., 2020) and Pt (II)-imprinted thiocyanato-functionalized SBA-15 (Dobrzynska et al., 2021) demonstrated outstanding adsorption capacity, their adsorption was performed at concentrations far higher than the actual environmental concentrations, and their removal efficiency for trace Pt-CDs remains unknown.

4. Conclusions

This study presents a comparative investigation of the adsorption behavior of trace cisplatin, carboplatin, and $PtCl_4^{2-}$ onto three different adsorbents, including studies on pH effect, adsorption kinetics, adsorption isotherms, and thermodynamic studies. Distinct adsorption mechanisms of each Pt compounds were revealed. The major findings of this study can be summarized as follows: (1) All three adsorbents exhibited a significant removal of anionic $PtCl_4^{2-}$ (>90 %) compared to cisplatin and carboplatin due to the assistance of electrostatic adsorption, however, the adsorption of $PtCl_4^{2-}$ is more pH dependent. Therefore, $PtCl_4^{2-}$ should be cautiously considered as a template for Pt-CDs, despite of structural similarity. (2) Si-Cys, containing thiol groups, exhibited a remarkable removal efficiency of cisplatin (maximum 76 ± 1 %), which is significantly higher than that of Si-DETA (maximum 34 ± 1 %) and Sponge (maximum 40 ± 5 %). And this similar contrast was also shown in the adsorption of carboplatin. It indicates the adsorption of cisplatin and carboplatin highly depends on the complexation with high-affinity thiol sites. (3) All the observed adsorption processes conform to the PSOM and Langmuir model descriptions, indicative of a monolayer chemisorption process. (4) The adsorption of cisplatin and carboplatin onto Si-Cys is an endothermic process (different from exothermic adsorption of $PtCl_4^{2-}$), as Pt—S binding is thermally favored. As a result, the removal of cisplatin and carboplatin onto Si-Cys reached 98.5 ± 0.1 % and 94.1 ± 0.1 %, respectively, when increasing the temperature up to 343 K. (5) The finding of treatment of Pt-spiked urine found that thiol-containing Si-Cys can be used to treat cisplatin and/or carboplatin-contained patient urine and hospital wastewater contaminated by it. In summary, our work provided ideas for the treatment of Pt-CDs contaminated wastewater and offered a strategy for dealing with this emerging and continuously deteriorating environmental threat that has been always neglected.

CRediT authorship contribution statement

Dong Han: Conceptualization, Methodology, Validation, Formal analysis, Investigation, Writing – original draft, Visualization. **Montserrat López-Mesas:** Conceptualization, Methodology, Resources, Writing – review & editing, Supervision, Project administration. **Markel Luaces:** Validation, Investigation, Writing – review & editing. **Yusleydi Enamorado:** Validation, Investigation, Writing – review & editing. **Martina Sanadar:** Methodology, Resources, Writing – review & editing. **Andrea Melchior:** Conceptualization, Methodology, Resources, Supervision, Writing – review & editing. **Manuel Valiente:** Conceptualization, Methodology, Resources, Project administration, Supervision, Funding acquisition.

Data availability

Data will be made available on request.

Declaration of competing interest

The authors declare that they have no known competing financial interests or personal relationships that could have appeared to influence the work reported in this paper.

Acknowledgements

This work has been developed in the framework of the European Community's H2020 Program H2020-MSCA-RISE 2017 under the project RECOPHARMA (grant agreement #778266). D. Han acknowledges COST action 18202, "Network for Equilibria and Chemical Thermodynamics Advanced Research" (NECTAR) for supporting a STSM in Udine and the program of China Scholarships Council (No. 201906450024). The authors would also like to thank Júlia Senyé Lacher, Tania Farías, Ana Rosa Lazo Fraga and Raquel Cantero Rodriguez for supporting in the experiment. Open Access funding provided thanks to the agreement CRUE-CSIC with Elsevier.

Appendix A. Supplementary data

Supplementary data to this article can be found online at https://doi.org/10.1016/j.scitotenv.2023.164385.

References

Abdulbur-Alfakhoury, E., Trommetter, G., Brion, N., Dumoulin, D., Reichstädter, M., Billon, G., Leermakers, M., Baeyens, W., 2021. Distribution of platinum (Pt), palladium (Pd), and rhodium (Rh) in urban tributaries of the Scheldt River assessed by diffusive gradients in thin films technique (DGT). Sci. Total Environ. 784, 147075. https://doi.org/10.1016/j.scitotenv.2021.147075.

Aitekenov, S., Gaipov, A., Bukasov, R., 2021. Review: detection and quantification of proteins in human urine. Talanta 223, 121718. https://doi.org/10.1016/j.talanta.2020.121718.

Araújo, A.P. da C., Mesak, C., Montalvão, M.F., Freitas, Í.N., Chagas, T.Q., Malafaia, G., 2019. Anti-cancer drugs in aquatic environment can cause cancer: insight about mutagenicity in tadpoles. Sci. Total Environ. 650, 2284–2293. https://doi.org/10.1016/J.SCITOTENV.2018.09.373.

Besse, J.P., Latour, J.F., Garric, J., 2012. Anticancer drugs in surface waters. What can we say about the occurrence and environmental significance of cytotoxic, cytostatic and endocrine therapy drugs? Environ. Int. 39, 73–86. https://doi.org/10.1016/j.envint.2011.10.002.

Bugarčić, Ž.D., Bogojeski, J., Petrović, B., Hochreuther, S., van Eldik, R., 2012. Mechanistic studies on the reactions of platinum(ii) complexes with nitrogen- and sulfur-donor biomolecules. Dalton Trans. 41, 12329. https://doi.org/10.1039/c2dt31045g.

Chinh, V.D., Hung, L.X., Di Palma, L., Hanh, V.T.H., Vilardi, G., 2019. Effect of carbon nanotubes and carbon nanotubes/gold nanoparticles composite on the photocatalytic activity of TiO2 and TiO2-SiO2. Chem. Eng. Technol. 42, 308–315. https://doi.org/10.1002/ceat.201800265.

Curtis, L., Turner, A., Vyas, N., Sewell, G., 2010. Speciation and reactivity of cisplatin in river water and seawater. Environ. Sci. Technol. 44, 3345–3350. https://doi.org/10.1021/es903620z.

Dobrzynska, J., Dabrowska, M., Olchowski, R., Zieba, E., Dobrowolski, R., 2021. Development of a method for removal of platinum from hospital wastewater by novel ion-imprinted mesoporous organosilica. J. Environ. Chem. Eng. 9. https://doi.org/10.1016/j.jece.2021.105302.

Farías, T., Hajizadeh, S., Ye, L., 2020. Cryogels with high cisplatin adsorption capacity: towards removal of cytotoxic drugs from wastewater. Sep. Purif. Technol. 235, 116203. https://doi.org/10.1016/j.seppur.2019.116203.

Feiqiang, G., Xiaolei, L., Xiaochen, J., Xingmin, Z., Chenglong, G., Zhonghao, R., 2018. Characteristics and toxic dye adsorption of magnetic activated carbon prepared from biomass waste by modified one-step synthesis. Coll. Surf. A Physicochem. Eng. Asp. 555, 43–54. https://doi.org/10.1016/j.colsurfa.2018.06.061.

Flores, C.R., Puga, M.P., Wrobel, Katarzyna, Garay Sevilla, M.E., Wrobel, Kazimierz, 2011. Trace elements status in diabetes mellitus type 2: possible role of the interaction between molybdenum and copper in the progress of typical complications. Diabetes Res. Clin. Pract. 91, 333–341. https://doi.org/10.1016/j.diabres.2010.12.014.

Folens, K., Abebe, A., Tang, J., Ronsse, F., Laing, G. Du, 2018. Biosorption of residual cisplatin, carboplatin and oxaliplatin antineoplastic drugs in urine after chemotherapy treatment. Environ. Chem. 15, 506–512. https://doi.org/10.1071/EN18115.

Fraguela, R.L., Ricardo, A., Edelia, M., Tagle, V., Sime, M., Alfonso, P., Cracchiolo, M., 2023. Evaluation of Dithiocarbamate-Modified Silica for Cisplatin Removal from Water 1–16.

Gao, Y., Yang, N., Yan, X., Hang, W., Xing, J., Zheng, J., Zhu, E., Huang, B., 2012. Early diagnosis of urinary lithiasis via elementary profile of serum samples. Anal. Methods 4, 693–698. https://doi.org/10.1039/c2ay05705k.

Ghafuri, Y., Yunesian, M., Nabizadeh, R., Mesdaghinia, A., Dehghani, M.H., Alimohammadi, M., 2018. Platinum cytotoxic drugs in the municipal wastewater and drinking water, a validation method and health risk assessment. Hum. Ecol. Risk. Assess. 24, 784–796. https://doi.org/10.1080/10807039.2017.1400372.

Ghafuria, Y., Yunesian, M., Nabizadeh, R., Mesdaghinia, A., Dehghani, M.H., Alimohammadi, M., 2018. Environmental risk assessment of platinum cytotoxic drugs: a focus on toxicity characterization of hospital effluents. Int. J. Environ. Sci. Technol. 15, 1983–1990. https://doi.org/10.1007/s13762-017-1517-6.

Gouveia, T.I.A., Silva, A.M.T., Freire, M.G., Sousa, A.C.A., Alves, A., Santos, M.S.F., 2023. Multi-target analysis of cytostatics in hospital effluents over a 9-month period. J. Hazard. Mater. 448, 130883. https://doi.org/10.1016/j.jhazmat.2023.130883.

Grumezescu, A.M., Ghitulica, C.D., Voicu, G., Huang, K.S., Yang, C.H., Ficai, A., Vasile, B.S., Grumezescu, V., Bleotu, C., Chifiriuc, M.C., 2014. New silica nanostructure for the improved delivery of topical antibiotics used in the treatment of staphylococcal cutaneous infections. Int. J. Pharm. 463, 170–176. https://doi.org/10.1016/j.ijpharm.2013.07.016.

Guo, W., Zhou, Q., Jia, Y., Xu, J., 2020. Cluster and factor analysis of elements in serum and urine of diabetic patients with peripheral neuropathy and healthy people. Biol. Trace Elem. Res. 194, 48–57. https://doi.org/10.1007/s12011-019-01747-x.

Han, D., Li, X., Gong, Z., Jiang, L., Wang, Z., Liu, P., 2021. Hierarchical porous catalytic pyrolysis char derived from oily sludge for enhanced adsorption. ACS Omega 6, 20549–20559. https://doi.org/10.1021/acsomega.1c02575.

Hann, S., Koellensperger, G., Stefánka, Z., Stingeder, G., Fürhacker, M., Buchberger, W., Mader, R.M., 2003. Application of HPLC-ICP-MS to speciation of cisplatin and its degradation products in water containing different chloride concentrations and in human urine. J. Anal. At. Spectrom. 18, 1391–1395. https://doi.org/10.1039/b309028k.

Heath, E., Isidori, M., 2020. Fate and Effects of Anticancer Drugs in the Environment, Fate and Effects of Anticancer Drugs in the Environment. Springer International Publishing, Cham https://doi.org/10.1007/978-3-030-21048-9.

Hernández, C., Ramos, Y., Fernández, L.A., Ledea, O., Bataller, M., Véliz, E., Besada, V., Rosado, A., 2008. Ozonation of cisplatin in aqueous solution at pH 9. Ozone Sci. Eng. 30, 189–196. https://doi.org/10.1080/01919510801907722.

Hirose, J., Kondo, F., Nakano, T., Kobayashi, T., Hiro, N., Ando, Y., Takenaka, H., Sano, K., 2005. Inactivation of antineoplastics in clinical wastewater by electrolysis. Chemosphere 60, 1018–1024. https://doi.org/10.1016/j.chemosphere.2005.01.024.

Hoffmann-La Roche, 2020. Product monograph Esbriet * product monograph [WWW document]. https://www.pfizer.ca/sites/default/files/202004/Cisplatin_PM_E_235278_2020-04-03.pdf.

Isidori, M., Lavorgna, M., Russo, C., Kundi, M., Žegura, B., Novak, M., Filipič, M., Mišík, M., Knasmueller, S., de Alda, M.L., Barceló, D., Žonja, B., Česen, M., Ščančar, J., Kosjek, T., Heath, E., 2016. Chemical and toxicological characterisation of anticancer drugs in hospital and municipal wastewaters from Slovenia and Spain. Environ. Pollut. 219, 275–287. https://doi.org/10.1016/j.envpol.2016.10.039.

Jantarat, T., Chuaychob, S., Thammakhet-Buranachai, C., Thavarungkul, P., Kanatharana, P., Srisintorn, W., Buranachai, C., 2021. A label-free DNA-based fluorescent sensor for cisplatin detection. Sensors Actuators B Chem. 326, 128764. https://doi.org/10.1016/j.snb.2020.128764.

Johnson, A.C., Oldenkamp, R., Dumont, E., Sumpter, J.P., 2013. Predicting concentrations of the cytostatic drugs cyclophosphamide, carboplatin, 5-fluorouracil, and capecitabine throughout the sewage effluents and surface waters of europe. Environ. Toxicol. Chem. 32, 1954–1961. https://doi.org/10.1002/etc.2311.

Jureczko, M., Kalka, J., 2020. Cytostatic pharmaceuticals as water contaminants. Eur. J. Pharmacol. 866, 172816. https://doi.org/10.1016/j.ejphar.2019.172816.

Kobayashi, T., Hirose, J., Sano, K., Hiro, N., Ijiri, Y., Takiuchi, H., Tamai, H., Takenaka, H., Tanaka, K., Nakano, T., 2008. Evaluation of an electrolysis apparatus for inactivating antineoplastics in clinical wastewater. Chemosphere 72, 659–665. https://doi.org/10.1016/j.chemosphere.2008.02.020.

Kümmerer, K., Helmers, E., Hubner, P., Mascart, G., Milandri, M., Reinthaler, F., Zwakenberg, M., 1999. European hospitals as a source for platinum in the environment in comparison with other sources. Sci. Total Environ. 225, 155–165. https://doi.org/10.1016/S0048-9697(98)00341-6.

Lenz, K., Hann, S., Koellensperger, G., Stefanka, Z., Stingeder, G., Weissenbacher, N., Mahnik, S.N., Fuerhacker, M., 2005. Presence of cancerostatic platinum compounds in hospital wastewater and possible elimination by adsorption to activated sludge. Sci. Total Environ. 345, 141–152. https://doi.org/10.1016/j.scitotenv.2004.11.007.

Lenz, K., Mahnik, S.N., Weissenbacher, N., Mader, R.M., Krenn, P., Hann, S., Koellensperger, G., Uhl, M., Knasmüller, S., Ferk, F., Bursch, W., Fuerhacker, M., 2007b. Monitoring, removal and risk assessment of cytostatic drugs in hospital wastewater. Water Sci. Technol. 56, 141–149. https://doi.org/10.2166/wst.2007.828.

Lenz, Katharina, Koellensperger, G., Hann, S., Weissenbacher, N., Mahnik, S.N., Fuerhacker, M., 2007a. Fate of cancerostatic platinum compounds in biological wastewater treatment of hospital effluents. Chemosphere 69, 1765–1774. https://doi.org/10.1016/j.chemosphere.2007.05.062.

Li, D., Chen, H., Liu, H., Schlenk, D., Mu, J., Lacorte, S., Ying, G.G., Xie, L., 2021. Anticancer drugs in the aquatic ecosystem: environmental occurrence, ecotoxicological effect and risk assessment. Environ. Int. 153, 106543. https://doi.org/10.1016/j.envint.2021.106543.

Li, J., Zhang, L.P., Peng, F., Bian, J., Yuan, T.Q., Xu, F., Sun, R.C., 2009. Microwave-assisted solvent-free acetylation of cellulose with acetic anhydride in the presence of iodine as a catalyst. Molecules 14, 3551–3566. https://doi.org/10.3390/molecules14093551.

Loehrer, P.J., 1984. Cisplatin. Ann. Intern. Med. 100, 704. https://doi.org/10.7326/0003-4819-100-5-704.

Lou, X.Y., Boada, R., Simonelli, L., Valiente, M., 2022a. Enhanced arsenite removal by superparamagnetic iron oxide nanoparticles in-situ synthesized on a commercial cube-shape sponge: adsorption-oxidation mechanism. J. Colloid Interface Sci. 614, 460–467. https://doi.org/10.1016/j.jcis.2022.01.119.

Lou, X.-Y., Boada, R., Verdugo, V., Simonelli, L., Pérez, G., Valiente, M., 2022b. Decoupling the adsorption mechanisms of arsenate at molecular level on modified cube-shaped sponge loaded superparamagnetic iron oxide nanoparticles. J. Environ. Sci. 121, 1–12. https://doi.org/10.1016/j.jes.2021.09.001.

Micanovic, R., Lafavers, K., Garimella, P.S., Wu, X.R., El-Achkar, T.M., 2020. Uromodulin (Tamm-Horsfall protein): Guardian of urinary and systemic homeostasis. Nephrol. Dial. Transplant. 35, 33–43. https://doi.org/10.1093/ndt/gfy394.

Mišík, M., Filipic, M., Nersesyan, A., Kundi, M., Isidori, M., Knasmueller, S., 2019. Environmental risk assessment of widely used anticancer drugs (5-fluorouracil, cisplatin, etoposide, imatinib mesylate). Water Res. 164, 114953. https://doi.org/10.1016/j.watres.2019.114953.

Mohan, D., Sarswat, A., Singh, V.K., Alexandre-Franco, M., Pittman, C.U., 2011. Development of magnetic activated carbon from almond shells for trinitrophenol removal from water. Chem. Eng. J. 172, 1111–1125. https://doi.org/10.1016/j.cej.2011.06.054.

Muñoz, J.A., Gonzalo, A., Valiente, M., 2002. Arsenic adsorption by Fe(III)-loaded open-celled cellulose sponge. Thermodynamic and selectivity aspects. Environ. Sci. Technol. 36, 3405–3411. https://doi.org/10.1021/es020017c.

Ogata, F., Inoue, K., Tominaga, H., Iwata, Y., Ueda, A., Tanaka, Y., Kawasaki, N., 2014. Use of calcined gibbsite to remove cisplatin from aqueous solutions. J. Water Environ. Technol. 12, 13–23. https://doi.org/10.2965/jwet.2014.13.

Patel, M., Kumar, R., Kishor, K., Mlsna, T., Pittman, C.U., Mohan, D., 2019. Pharmaceuticals of emerging concern in aquatic systems: chemistry, occurrence, effects, and removal methods. Chem. Rev. 119, 3510–3673. https://doi.org/10.1021/acs.chemrev.8b00299.

Pieczyńska, A., Borzyszkowska, A.F., Ofiarska, A., Siedlecka, E.M., 2017. Removal of cytostatic drugs by AOPs: a review of applied processes in the context of green technology. Crit. Rev. Environ. Sci. Technol. 47, 1282–1335. https://doi.org/10.1080/10643389.2017.1370990.

Prestayko, A.W., D'Aoust, J.C., Issell, B.F., Crooke, S.T., 1979. Cisplatin (cis-diamminedichloroplatinum II). Cancer Treat. Rev. 6, 17–39. https://doi.org/10.1016/S0305-7372(79)80057-2.

Queirós, V., Azeiteiro, U.M., Soares, A.M.V.M., Freitas, R., 2021. The antineoplastic drugs cyclophosphamide and cisplatin in the aquatic environment – review. J. Hazard. Mater. 412. https://doi.org/10.1016/j.jhazmat.2020.125028.

Reedijk, J., 1999. Why does cisplatin reach guanine-N7 with competing S-donor ligands available in the cell? Chem. Rev. 99, 2499–2510. https://doi.org/10.1021/cr980422f.

Reedijk, J., 2009. Platinum anticancer coordination compounds: study of DNA binding inspires new drug design. Eur. J. Inorg. Chem. 1303–1312. https://doi.org/10.1002/ejic.200900054.

Roque-Diaz, Y., Sanadar, M., Han, D., López-Mesas, M., Valiente, M., Tolazzi, M., Melchior, A., Veclani, D., 2021. The dark side of platinum based cytostatic drugs: from detection to removal. Processes 9, 1873. https://doi.org/10.3390/pr9111873.

Santana-Viera, S., Padrón, M.E.T., Sosa-Ferrera, Z., Santana-Rodríguez, J.J., 2020. Quantification of cytostatic platinum compounds in wastewater by inductively coupled plasma mass spectrometry after ion exchange extraction. Microchem. J. 157, 104862. https://doi.org/10.1016/j.microc.2020.104862.

Schmidt, C.W.P., 2019. Pediatric Oncologic Pharmacy. Springer International Publishing, Cham, Pediatric Oncologic Pharmacy https://doi.org/10.1007/978-3-030-10988-2.

Sen Gupta, S., Bhattacharyya, K.G., 2011. Kinetics of adsorption of metal ions on inorganic materials: a review. Adv. Colloid Interf. Sci. 162, 39–58. https://doi.org/10.1016/j.cis.2010.12.004.

Veclani, D., Tolazzi, M., Melchior, A., 2020. Molecular interpretation of pharmaceuticals' adsorption on carbon nanomaterials: theory meets experiments. Processes 8, 1–39. https://doi.org/10.3390/PR8060642.

Villarini, M., Gianfredi, V., Levorato, S., Vannini, S., Salvatori, T., Moretti, M., 2016. Occupational exposure to cytostatic/antineoplastic drugs and cytogenetic damage measured using the lymphocyte cytokinesis-block micronucleus assay: a systematic review of the literature and meta-analysis. Mutat. Res. Rev. Mutat. Res. 770, 35–45. https://doi.org/10.1016/j.mrrev.2016.05.001.

Vyas, N., Turner, A., Sewell, G., 2014. Platinum-based anticancer drugs in waste waters of a major UK hospital and predicted concentrations in recipient surface waters. Sci. Total Environ. 493, 324–329. https://doi.org/10.1016/j.scitotenv.2014.05.127.

Wang, J., Guo, X., 2020a. Adsorption kinetic models: physical meanings, applications, and solving methods. J. Hazard. Mater. 390, 122156. https://doi.org/10.1016/j.jhazmat.2020.122156.

Wang, J., Guo, X., 2020b. Adsorption isotherm models: classification, physical meaning, application and solving method. Chemosphere 258, 127279. https://doi.org/10.1016/j.chemosphere.2020.127279.

Yadav, A., Rene, E.R., Mandal, M.K., Dubey, K.K., 2021. Threat and sustainable technological solution for antineoplastic drugs pollution: review on a persisting global issue. Chemosphere 263, 128285. https://doi.org/10.1016/j.chemosphere.2020.128285.

Zamble, D.B., Lippard, S.J., 1995. Cisplatin and DNA repair in cancer chemotherapy. Trends Biochem. Sci. 20, 435–439. https://doi.org/10.1016/S0968-0004(00)89095-7.